

# Direct Evidence for Metabolon Formation and Substrate Channeling in Recombinant TCA Cycle Enzymes

Beyza Bulutoglu<sup>1,4</sup>, Kristen E. Garcia<sup>1,4</sup>, Fei Wu<sup>2,3,4</sup>, Shelley D. Minter<sup>2</sup> and Scott Banta<sup>1\*</sup>

<sup>1</sup> Department of Chemical Engineering, Columbia University, New York, NY, 10027, United States

<sup>2</sup> Department of Chemistry, The University of Utah, Salt Lake City, UT, 84112, United States

<sup>3</sup> Institute of Chemistry, Chinese Academy of Science, Beijing, China

<sup>4</sup> These authors contributed equally to this work.

\*To whom correspondence should be addressed.

Scott Banta, e-mail: sbanta@columbia.edu, telephone number: +1 212-854-7531

# Table of Contents

- I. Supplemental Figures
- II. Supplemental Tables
- III. Materials and Methods
  - a. Genes, chemicals and bacterial strains
  - b. Construction, expression and purification of enzymes
    - i. Cloning of synthetic genes into expression plasmids
    - ii. Site-directed mutagenesis of recombinant CS
    - iii. Expression and purification of recombinant enzymes
    - iv. Preparation of crude mitochondrial lysate
  - c. Structural analysis
    - i. *In vitro* chemical cross-linking of mMDH, CS and Aco
    - ii. Separation and in-gel digestion of enzyme complexes
    - iii. Mass spectrometric instrumentation
    - iv. Mascot database searches
    - v. Identification of cross-linked peptides
    - vi. Hybrid protein docking
    - vii. Simulation of the electrostatic surface potential
  - d. Kinetic analysis
    - i. Kinetic analysis of recombinant enzymes
    - ii. Coupled activity assays of the mMDH-CS complex in solution with aspartate aminotransferase (AAT) or glycerol
    - iii. Coupled activity assay of immobilized mMDH-CS complex with AAT
    - iv. Transient time measured by fast kinetic study
    - v. Predicted transient time calculations
    - vi. Elasticity coefficient calculations
- IV. References

## I. Supporting Figures

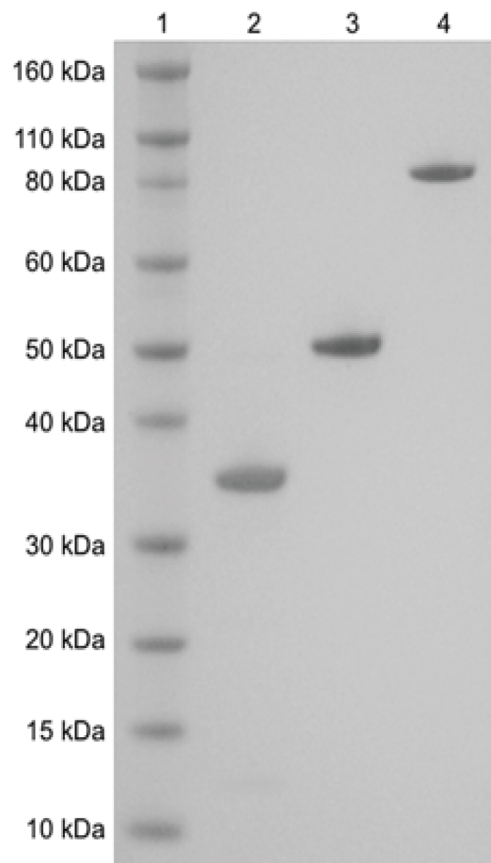


**Figure S1.** SDS-PAGE analysis of recombinant enzymes. (1) Protein ladder. (2) mMDH - 34 kDa. (3) CS - 49 kDa. (4) Aco - 85 kDa.

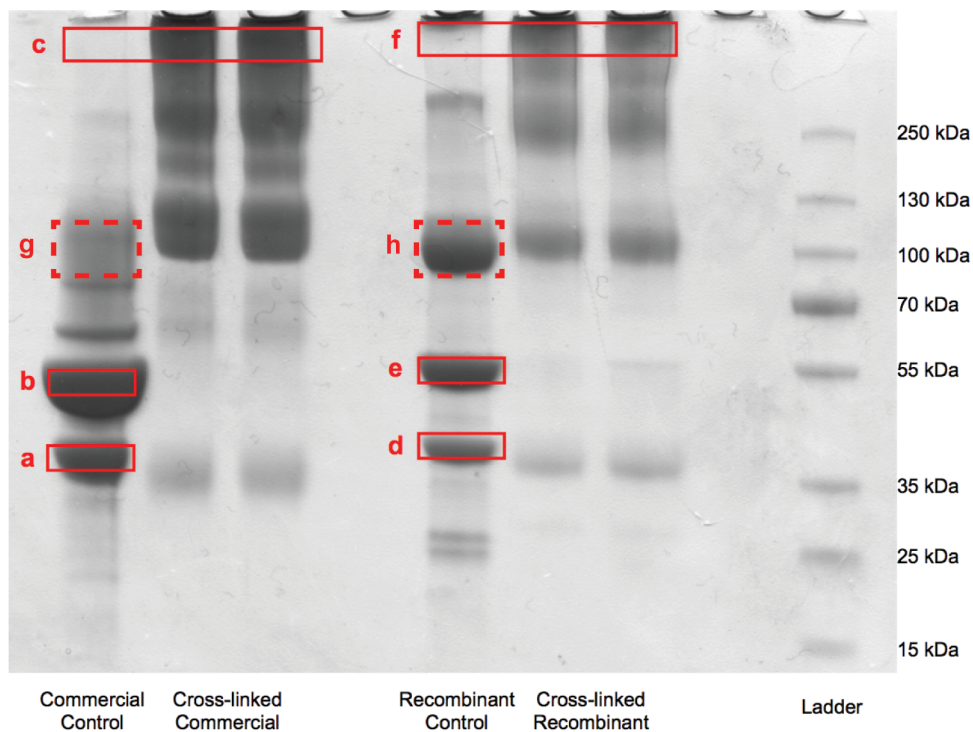


**Figure S2.** SDS-PAGE analysis of DSG-cross-linked and non-cross-linked (control) mMDH-CS complexes *in vitro* for commercial and recombinant enzymes. (a) Commercial mMDH subunit. (b) Commercial CS subunit. (c) Commercial mMDH-CS complex. (d) Recombinant mMDH subunit. (e) Recombinant CS subunit. (f) Recombinant mMDH-CS complex. (g) Commercial Aco. (h) Recombinant Aco. Gel bands of interest for subsequent digestion and analysis are indicated by solid red squares.

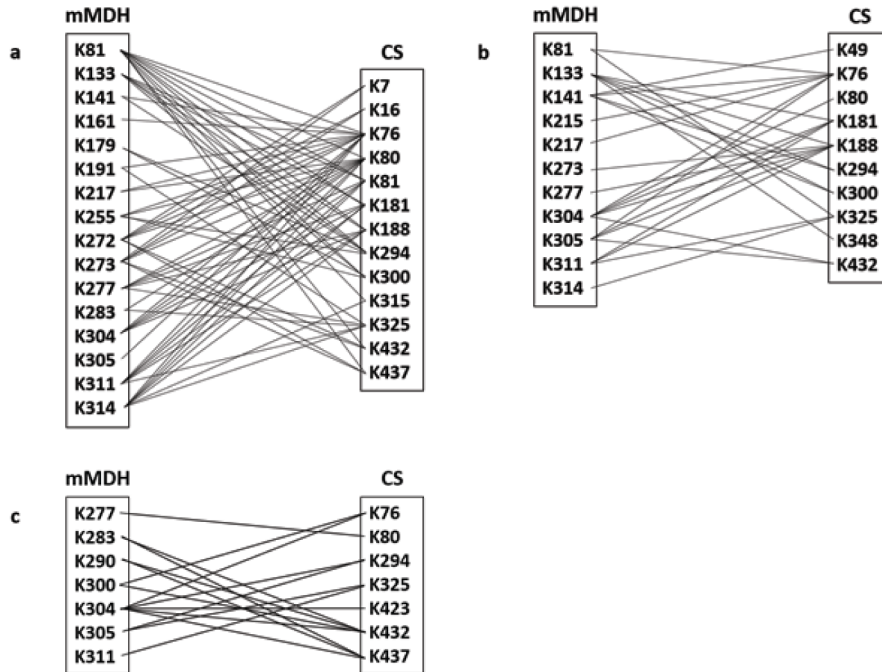


**Figure S3.** Summary of all possibly cross-linked lysine residues (represented by K) (a) in the *in vitro* mMDH-CS complex formed by commercially available enzymes. (b) in the *in vitro* mMDH-CS complex formed by recombinant enzymes. (c) in the *in vivo* mMDH-CS complex formed by native tissue mitochondrial enzymes.

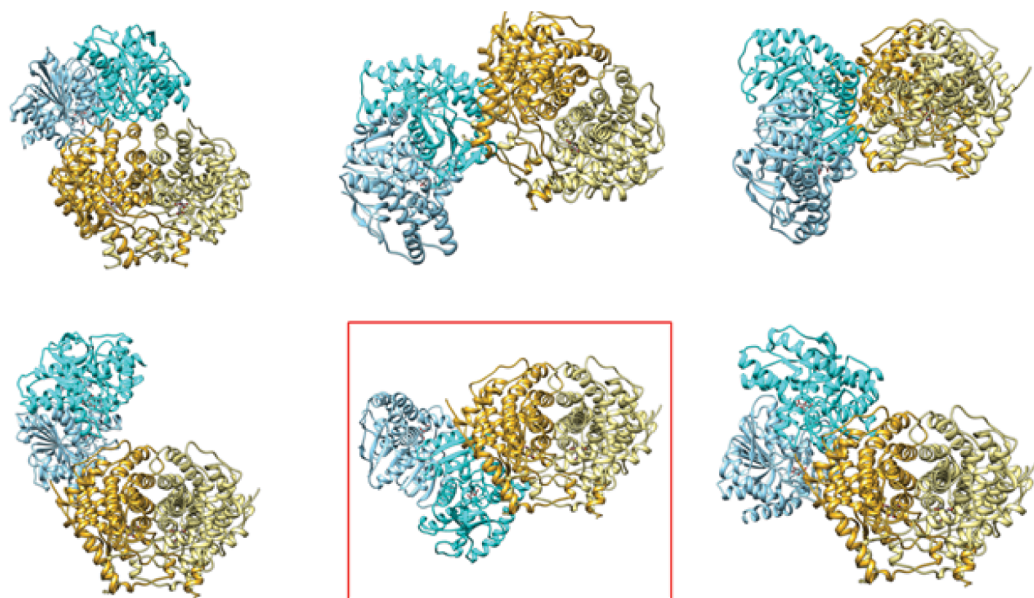


**Figure S4.** mMDH-CS metabolon structures. All possible complex structures formed by commercial mMDH (colored in sky blue and cyan) and CS (colored in gold and yellow) in solution. The crystal structures of mMDH and CS were obtained from the Protein Data Bank (PDB ID: 1MLD and 1CTS). The structure with the most similarity to the natural metabolon is highlighted in the red square.

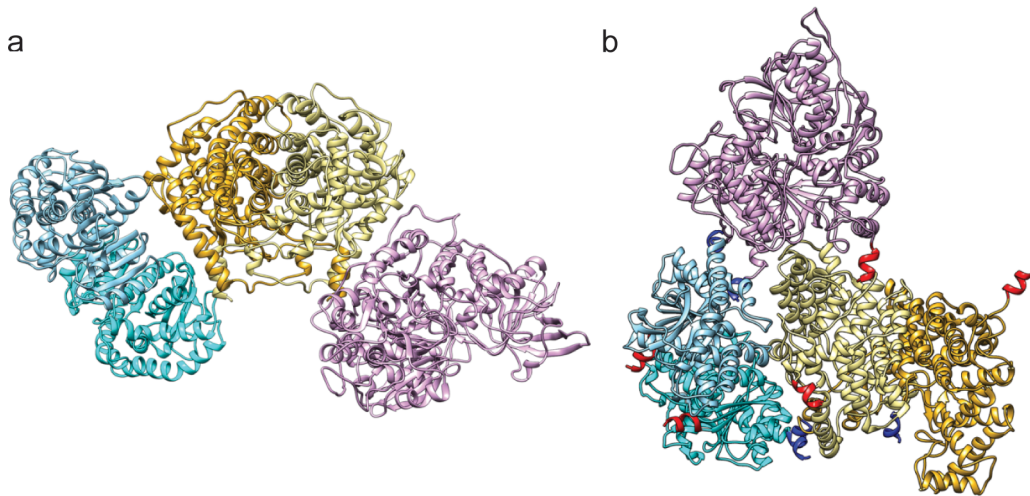


**Figure S5.** mMDH-CS-Aco complex structures. **(a)** Structures of the complex of commercial enzymes and **(b)** recombinant mMDH-CS-Aco complexes formed *in vitro*. The crystal structures of mMDH, CS and Aco were obtained from the Protein Data Bank (PDB ID: 1MLD, 1CTS, and 7ACN). Aco is colored in purple. FLAG-tagged N-terminus and His-tagged C-terminus are highlighted in red and blue, respectively.

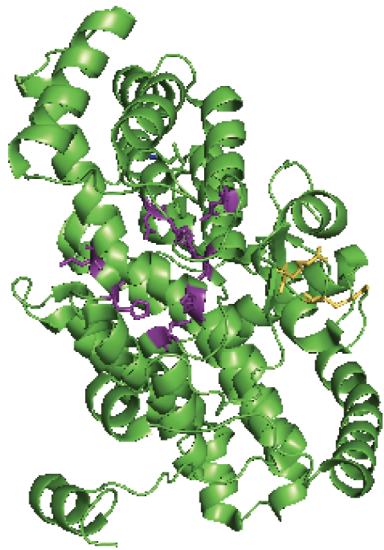


**Figure S6.** Location of mutations in CS. Structure of a porcine CS subunit (PDB ID: 1CTS). The residues shown in purple represent the mutation sites found in literature (Table S6).<sup>1,2</sup> The residues shown in yellow represent the Arg65 and Arg67 positions.

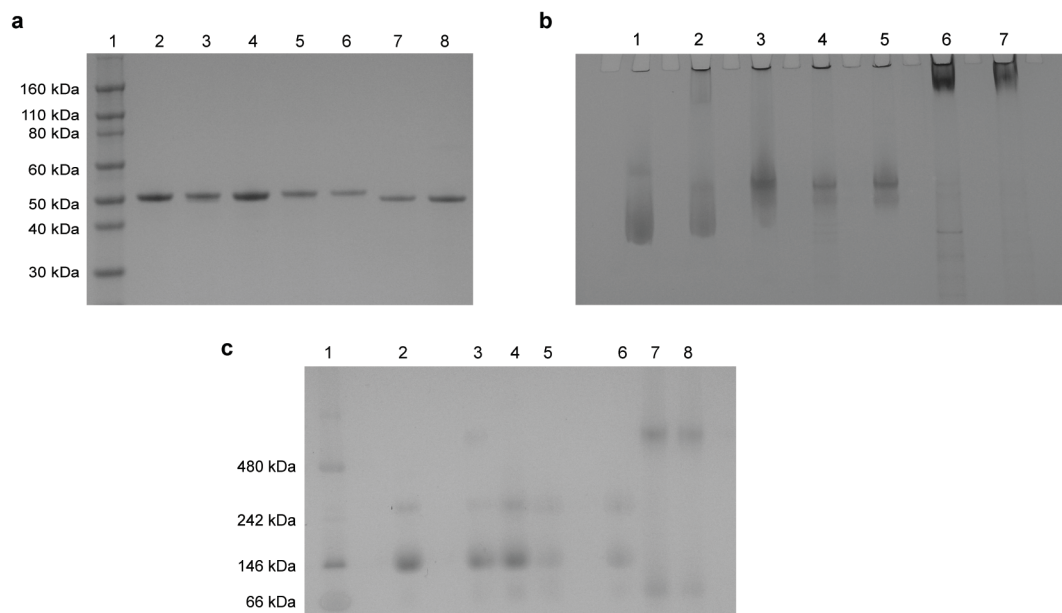


**Figure S7.** Protein gel pictures of CS mutants. **(a)** SDS-PAGE analysis: (1) Protein ladder. (2) recombinant CS. (3) CS(R65A). (4) CS(R67A). (5) CS(R65A/R67A). (6) CS(R65D). (7) CS(R67D). (8) CS(R65D/R67D). All mutants have a molecular weight of 49 kDa. **(b)** Native-PAGE analysis: (1) Recombinant CS. (2) CS(R65A). (3) CS(R67A). (4) CS(R65A/R67A). (5) CS(R65D). (6) CS(R67D). (7) CS(R65D/R67D). **(c)** Blue Native-PAGE analysis: (1) Protein ladder. (2) Recombinant CS. (3) CS(R65A). (4) CS(R67A). (5) CS(R65A/R67A). (6) CS(R65D). (7) CS(R67D). (8) CS(R65D/R67D).

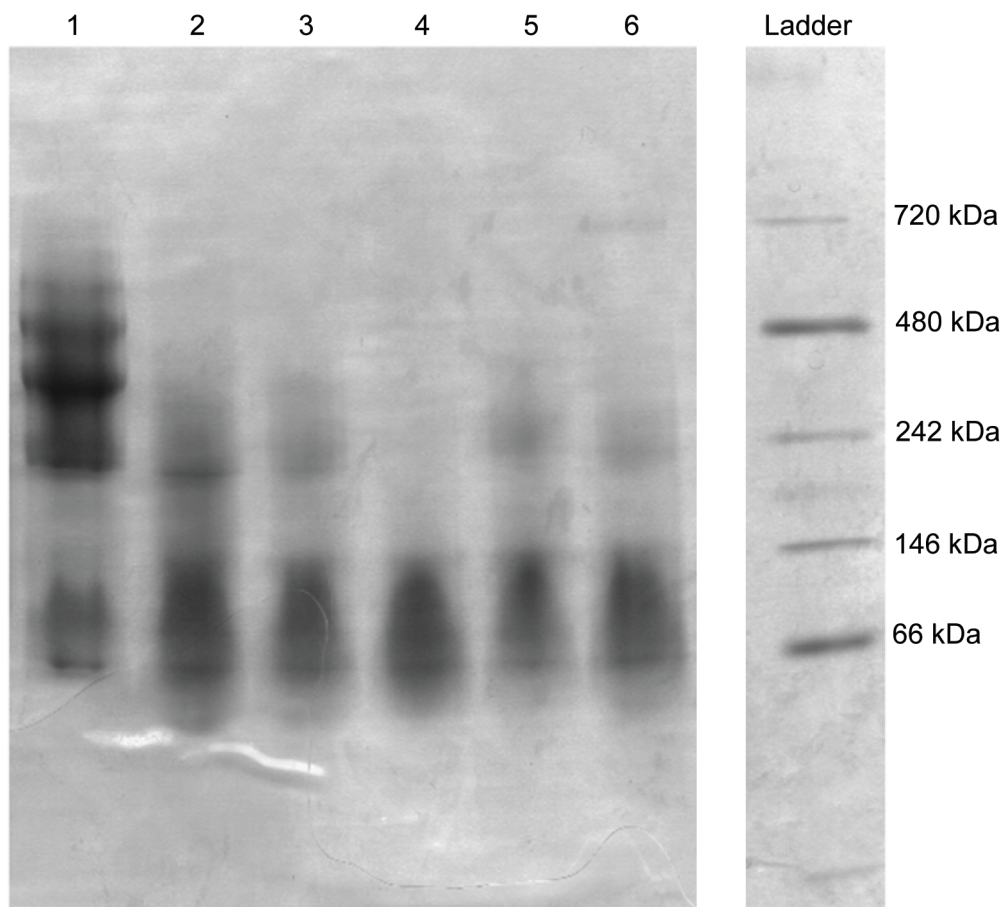


**Figure S8.** Blue Native-PAGE analysis. (1) Recombinant mMDH-CS complex. (2) Recombinant mMDH-CS(R65D) complex. (3) Recombinant mMDH-CS(R67A) complex. (4) Recombinant mMDH-CS(R67D) complex. (5) Recombinant mMDH-CS(R65A) complex. (6) Recombinant mMDH-CS(R65A/R67A) complex. (7) Protein ladder. All complexes were at 20  $\mu$ M.

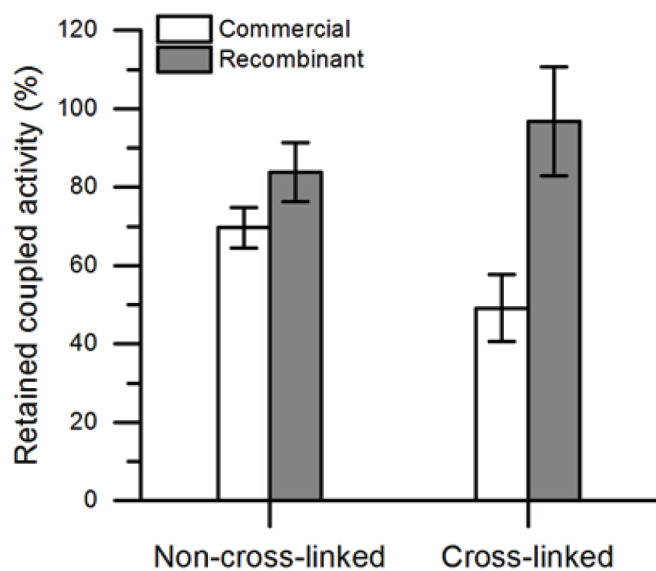


**Figure S9.** Coupled activity retention of the commercial and recombinant mMDH-CS complexes immobilized in chitosan in the presence of  $1 \text{ U mL}^{-1}$  AAT. Error bars represent standard deviation calculated from three independent experiments.

## II. Supporting Tables

**Table S1.** Identified Krebs cycle enzymes in the cross-linked and non-cross-linked (control) protein bands based on Mascot search results (mass tolerance: 5 ppm). Same sequences matched to database with variable modifications were counted as one unique peptide.

Band name	Enzyme name	Score	Queries matched	Unique peptides	Sequence coverage
Non-cross-linked commercial	mMDH	1598	162	32	67%
	CS	893	63	17	25%
	Aco	805	32	20	30%
Cross-linked commercial	mMDH	782	172	12	44%
	CS	557	424	10	22%
	Aco	97	3	2	3%
Non-cross-linked recombinant	mMDH	826	42	14	48%
	CS	831	96	16	30%
	Aco	2672	197	56	52%
Cross-linked recombinant	mMDH	507	16	9	35%
	CS	449	35	10	18%
	Aco	1223	69	26	32%

**Table S2.** List of identified DSG cross-linked peptides from complexes of commercially purchased mMDH and CS

mMDH	CS	m/z	M(expt.)	M(calc.)	Mass error (ppm)
GIEK <sup>K</sup> NLGIGK(HDSG)ISPFEEK or GIEK(HDSG)NLGIG <sup>K</sup> ISPFEEK	KTDPRYTC(PAM)QR	1136.2471	3405.7230	3405.7239	-0.26
TIIP LISQCTP <sup>K</sup> VDFPQDQLSTLTGR	KTDPRYTCQR	1059.2951	4233.1512	4233.1561	-1.16

**Table S3.** List of identified DSG-cross-linked peptides in the recombinant mMDH-CS complex

mMDH	CS	m/z	M(expt.)	M(calc.)	Mass error (ppm)
GC(PAM)DVVVIPAGVPR KPGM(OX)TR	KTDPR	917.4877	2749.4412	2749.4366	1.67
ASIK <sup>K</sup> (HDSG)GEEFVK or ASIK(HDSG) <sup>K</sup> GEEFVK	SM(OX)STDGLIKLVDSK	985.5126	2953.5159	2953.5208	-2.78
GC(PAM)DVVVIPAGVPR KPGMTR	FRGYSIPEC(PAM)Q <sup>K</sup> MLP K	997.2728	3985.0620	3985.0559	1.08
IQEAGTEVV <sup>K</sup> AK(HDSG) AGAGSATLSMAYAGAR or IQEAGTEVV <sup>K</sup> AK(HDSG) AGAGSATLSMAYAGAR	GYSIPEC(CAD)Q <sup>K</sup> M(OX)L PK	874.8433	4369.1800	4369.1740	1.73
IQEAGTEVV <sup>K</sup> AK(HDSG) AGAGSATLSM(OX)AYAG AR or IQEAGTEVV <sup>K</sup> AK(HDSG) AGAGSATLSM(OX)AYAG AR	GYSIPEC(CAD)Q <sup>K</sup> M LPK				

**Table S4.** List of identified DSG cross-links of commercial Aco and CS

Aco peptide	CS peptide	m/z	M (expt.)	M (calc.)	Mass error (ppm)
RAK <b>D</b> INQEVYNFLATAGAK	GYSIPECQ <b>K</b> M(OX)LPK	929.2218	3712.858 0	3712.859 2	-0.32
AKVAMSHFEPHE <b>I</b> RYDLL EK	DILADLIP <b>K</b> EQAR	1039.038 6	4152.125 2	4152.135 1	-2.38
AK <b>D</b> INQEVYNFLATAGAK	GYSIPEC(CAD)Q <b>K</b> M(OX)LP KAK	954.2368	3812.918 0	3812.910 1	2.07

**Table S5.** List of identified DSG cross-links of recombinant Aco and CS

Aco peptide	CS peptide	m/z	M (expt.)	M (calc.)	Mass error (ppm)
DFAPG <b>K</b> PCIIK or DFAPGKPCII <b>K</b>	EVG <b>K</b> DVSDEKLR or EVGKDVSDE <b>K</b> LR	967.1876	2898.5409	2898.5520	-3.83

**Table S6.** CS mutations found in literature

Residue	Mutations	Location
H235 <sup>a</sup>	Q	
N242 <sup>a</sup>	E	
H274 <sup>b</sup>	G, R	OAA / acetyl-CoA binding site
G275 <sup>a</sup>	A, V	
H320 <sup>a</sup>	R, N, Q, G	OAA binding site
D327 <sup>a</sup>	N	
D375 <sup>b</sup>	N, Q, E, G	acetyl-CoA binding site
R401 <sup>a</sup>	G, H, K	OAA binding site

<sup>a</sup> Evans, *et al.*<sup>1</sup> <sup>b</sup> Alter, *et al.*<sup>2</sup>

**Table S7.** Kinetic properties of recombinant CS mutants <sup>a</sup>

Enzyme	Enzyme Concentration (nM)	Specific Activity (s <sup>-1</sup> )	Relative Specific Activity
Recombinant CS	3	28.5	1.00
CS(R65A)	3	24.5	0.86
CS(R67A)	300	0.59	0.02
CS(R65A/R67A)	3000	0.12	0.004
CS(R65D)	300	0.24	0.008
CS(R67D)		N/A	
CS(R65D/R67D)		N/A	

<sup>a</sup>The specific activities were measured in 50 mM Tris-HCl (pH 7.7) with 0.2 mM acetyl-CoA, 0.5 mM OAA and 1 mM DTNB.

**Table S8.** Conservation of Arg65 and Arg67 in CS <sup>a</sup>

Organism	Sequence ID	Match (%)	Residue at Position 65 / 67
Capitella teleta	ELU15766.1	76	E / R
Metaseiulus occidentalis	XP_003739390.1	73	A / R
Ixodes scapularis	XP_002411280.1	73	A / R
Sarcoptes scabiei	KPM02928.1	73	S / R
Limulus polyphemus	XP_013775370.1	72	E / R
Nematostella vectensis	XP_001641037.1	72	E / R
Stegodyphus mimosarum	KFM64927.1	68	E / R
Rhizophagus irregularis	EXX70579.1	65	E / R

<sup>a</sup>The data includes the mismatches between CS Arg65 and Arg67 among the first 500 hits obtained via Basic Local Alignment Search Tool.<sup>3</sup> Sequence identity varied between 64 – 100% for the search.

**Table S9.** Primers used to perform site-directed mutagenesis on CS

Mutation	Primer	Sequence
CS(R65A)	Forward	5' CGGACGAAGGCATTGCTTTTCGCGGTTATTC 3'
	Reverse	5' GAATAACCGCGAAAAGCAATGCCTTCGTCCG 3'
CS(R67A)	Forward	5' GAAGGCATTGCTTTTGCCGTTATTCGATCCC 3'
	Reverse	5' GGGATCGAATAACCGGCAAAACGAATGCCTTC 3'
CS(R65D)	Forward	5' CCGGACGAAGGCATTGATTTTCGCGGTTATTCG 3'
	Reverse	5' CGAATAACCGCGAAAATCAATGCCTTCGTCCGG 3'
CS(R67D)	Forward	5' CGAAGGCATTGCTTTTGACGGTTATTCGATCCC 3'
	Reverse	5' GGGATCGAATAACCGTCAAAACGAATGCCTTCG 3'
CS(R65A/R67A)	Forward	5' GAAGGCATTGCTTTTGCCGTTATTCGATCCC 3'
	Reverse	5' GGGATCGAATAACCGGCAAAAGCAATGCCT TC 3'
CS(R65D/67D)	Forward	5' CGAAGGCATTGATTTTGACGGTTATTCGATCCCC 3'
	Reverse	5' CGGGATCGAATAACCGTCAAAATCAATGCCTTCG 3'

### **III. Materials and Methods**

#### **a. Genes, chemicals and bacterial strains**

Synthetic genes coding for the porcine heart enzymes were synthesized by Genscript. All genes have a Flag-tag at the N-terminus and a 6xHis-tag at the C-terminus, for identification and purification purposes, respectively. Restriction enzymes for DNA cloning were purchased from New England Biolabs. Isopropyl  $\beta$ -D-1-thiogalactopyranoside (IPTG) and ampicillin sodium salt, were purchased from Gold Biotechnology. Amicon centrifugal filters were purchased from Millipore. Disuccinimidyl glutarate (DSG), sodium dodecyl sulfate polyacrylamide electrophoresis gels (SDS-PAGE) and running buffers were purchased from Invitrogen-Life Technologies. *E. coli* BL21 and BL21(DE3) cell lines were purchased from Bioline. Chaperon plasmid pGro7 was purchased from Clontech Laboratories-Takara. Alachitosan was prepared as previously described.<sup>4</sup> Fresh bovine heart was purchased from a local slaughterhouse and used immediately. All other reagents and materials were purchased from Sigma-Aldrich unless otherwise stated.

#### **b. Construction, expression and purification of enzymes**

##### **i. Cloning of the synthetic genes into expression plasmids**

The genes coding for CS and Aco were cloned into pET-20b(+) backbone using the NdeI and HindIII restriction sites. Resulting plasmids were transformed into BL21(DE3) cells. mMDH was inserted into pMAL-c4e expression vector via the same restriction sites. The resulting construct and the chaperon plasmid pGro7 were co-transformed into BL21 cells for expression.

##### **ii. Site-directed mutagenesis of recombinant CS**

CS Arg65 and Arg67 were mutated to alanine and aspartic acid to create single and double mutants via site-directed mutagenesis: CS(R65A), CS(R67A), CS(R65A/R67A), CS(R65D), CS(R67D), CS(R65D/R67D). CS(R65A) was used as the template to mutate the Arg67 to alanine and CS(R65D) was used as the template to mutate Arg67 to aspartic acid. Corresponding primer sequences used during the PCR reaction are given in Table S9.

##### **iii. Expression and purification of the recombinant enzymes**

All constructs were expressed in 1L of sterilized Terrific Broth, inoculated with 10 ml overnight culture. For Aco and CS, the media was supplemented with 100  $\mu\text{g mL}^{-1}$  ampicillin. 35  $\mu\text{g mL}^{-1}$  chloramphenicol was added to mMDH cultures in addition to the ampicillin. The cells were grown to an  $\text{OD}_{600}$  of 0.6 while shaking at 37°C, and protein

expression was induced with 0.5 mM IPTG for mMDH and CS, and with 0.6mM IPTG for Aco. Expression was carried out for 18-20 h at 25 °C. Cells were harvested by centrifugation at 5000 × g for 10 min and resuspended in 50 mL HisTrap binding buffer (20 mM Tris, 150 mM NaCl and 20 mM imidazole, pH 7.4) per L of culture. Soluble proteins were collected via centrifugation at 15000 × g for 30 min after the cells were lysed by sonication with an ultrasonication probe in an ice bath for 6 min (5 s on pulse and 2 s off pulse). Enzymes of interest were purified by immobilized metal affinity chromatography using HisTrap columns (GE Healthcare Life Sciences), where bound enzymes were eluted with the elution buffer (20 mM Tris, 150 mM NaCl, 500 mM imidazole (pH 7.4). mMDH was buffer exchanged into 20 mM Tris-HCl (pH 8.7) and purified via anion exchange chromatography where the enzyme was eluted using a linear NaCl gradient from 0 to 1 M NaCl. All enzymes were further purified with size exclusion chromatography after buffer exchanging into 50 mM Tris, 150 mM NaCl (pH 7.4). Amicon filters (Milipore) with 30 kDa (for mMDH and CS) and 50 kDa (for Aco) molecular weight cutoff were used in order to concentrate the protein solutions as well as to exchange the buffer in between different purification steps.

#### **iv. Preparation of crude mitochondrial lysate**

Extraction of the bovine heart mitochondria was done according to the procedure described by Rogers *et al.* with some modifications.<sup>5</sup> Bovine heart cubes were blended with cold isolation buffer (70 mM sucrose, 210 mM mannitol, 5 mM HEPES, 1 mM EGTA and 0.5% (w/v) BSA, pH 7.2) in a Waring laboratory blender. Meat suspension was centrifuged at 500 × g for 10 min, and the supernatant was centrifuged at 26000 × g for 20 min. Pellet was homogenized in the isolation buffer and centrifuged twice again at 500 × g for 10 min. Supernatant was filtered through a double-layer cheesecloth and centrifuged at 1000 × g for 20 min. The mitochondria pellet was washed with lysis buffer (50 mM Tris, 150 mM NaCl, 2 mM EDTA and 1 mM PMSF, pH 7.4) at 26000 × g for 10 min. Pellet resuspended in the lysis buffer was sonicated with an ultrasonication probe in ice bath for 4 min (5 s on pulse and 15 s off pulse). The crude lysate was initially cleared at 5000 × g for 30 min. EDTA and PMSF were removed through the pre-packed Sephadex™ G-25M column. Protein concentration in the mitochondrial lysate was determined to be 1 mg mL<sup>-1</sup> by BCA assay.

#### **c. Structural analysis**

##### **i. *In vitro* chemical cross-linking of mMDH, CS and Aco**

Commercially available enzymes purchased from Sigma-Adrich and recombinant enzymes were cleaned up by a pre-packed Sephadex™ G-25M column (GE Healthcare) into 10 mM phosphate buffer (pH 7.4) to remove ammonium sulfate and other salts containing primary amine. Afterwards, mMDH, CS and Aco were mixed equally to a total protein concentration

of 20  $\mu\text{M}$  in 10 mM phosphate buffer (pH 7.4). DSG dissolved in 50  $\mu\text{L}$  of DMF was added to the enzyme mixture to a final concentration of 1 mM. The approximate DSG/protein molar ratio was 50:1 to ensure an efficient capture of weak protein-protein interactions in dilute solution without dramatic loss of enzyme activity. As the non-cross-linked control, 50  $\mu\text{L}$  of DMF containing no DSG was used. Cross-linking was carried out at room temperature for 30 min under gentle shaking and quenched by adding 2 M Tris buffer (pH 8.3) to a final concentration of 20 mM.

## **ii. Separation and in-gel digestion of enzyme complexes**

Enzyme mixtures were washed with 50 mM Tris buffer (pH 7.4) in filter-incorporated Amicon tubes with a mass cutoff at 10 kDa (Millipore) at  $5000 \times g$  for 15 min to remove phosphates and extra DSG. Afterwards, cross-linked and non-cross-linked samples were directly separated by reducing SDS-PAGE, which was performed on a 4–20% gradient gel according to the protocol provided by the manufacturer. Gel bands of interest were excised and de-stained twice in 1 mL of 50% methanol with 50 mM ammonium bicarbonate at room temperature, under gentle vortexing for 1 h. The gel slices were rehydrated in 1 mL of 50 mM ammonium bicarbonate at room temperature for 30 min, and the gel bands/spots of interest were cut into several pieces. These gel pieces were rehydrated in 1 mL of 100% acetonitrile at room temperature under gentle shaking for 30 min. Acetonitrile was carefully removed from the gel pieces with a pipette tip prior to trypsin digestion. The gel pieces were incubated with 10–20  $\mu\text{L}$  of sequence-grade modified trypsin (20  $\text{ng } \mu\text{L}^{-1}$ , Promega) in 50 mM ammonium bicarbonate overnight at 37  $^{\circ}\text{C}$ . Digestion was quenched by adding 20  $\mu\text{L}$  of 1% formic acid. Then, the solution was allowed to stand, and peptides that dissolved in the 1% formic solution were extracted and collected. Further extraction of peptides from the gel material was performed twice by adding 50% acetonitrile with 1% formic acid and sonicating at 37  $^{\circ}\text{C}$  for 20 min. All these solutions were collected and combined. A final complete dehydration of the gel pieces was accomplished by adding 20  $\mu\text{L}$  of 100% acetonitrile followed by incubation at 37  $^{\circ}\text{C}$  for 20 min. The combined supernatant solutions of extracted peptides were dried in a vacuum centrifuge (Speed-Vac). The peptides were reconstituted in 100  $\mu\text{L}$  of 5% acetonitrile with 0.1% formic acid for mass spectrometric analysis.

## **iii. Mass spectrometric instrumentation**

Peptides were analyzed using a nano-liquid chromatography-tandem mass spectrometry (LC-MS/MS) system comprised of a nano-LC pump (Eksigent) and a LTQ-FT mass spectrometer (ThermoElectron Corporation). The LTQ-FT is a hybrid mass spectrometer with a linear ion trap used typically for MS/MS fragmentation (i.e. peptide sequence) and a Fourier transform ion-cyclotron resonance (FT-ICR) mass spectrometer used for primary accurate mass measurement of peptide ions. The LTQ-FT is equipped with a nanospray ion source (ThermoElectron Corporation). Approximately 5 to 20 fM of tryptic-digested or

phosphopeptide-enriched samples were dissolved in 5% acetonitrile with 0.1% formic acid and injected onto a homemade C18 nanobore LC column for nano-LC-MS/MS. A linear gradient LC profile was used to separate and elute peptides, consisting of 5 to 70% solvent B in 78 min with a flow rate of 350 nL min<sup>-1</sup> (solvent A: 5% acetonitrile with 0.1% formic acid; solvent B: 80% acetonitrile with 0.1% formic acid). The LTQ-FT mass spectrometer was operated in the data-dependent acquisition mode controlled by *Xcalibur 1.4* software, in which the “top 10” most intense peaks observed in an FT primary scan (i.e. MS survey spectrum) were determined by the computer on-the-fly and each peak was subsequently trapped for MS/MS analysis and sequenced through peptide fragmentation by collision-induced dissociation. Spectra in the FT-ICR were acquired from m/z 400 to 1700 at 50000 resolving power with about 3 ppm mass accuracy. The LTQ linear ion trap was operated with the following parameters: precursor activation time was 30 ms and activation Q was 0.25; collision energy was set at 35%; dynamic exclusion width was set at low mass of 0.1 Da with one repeat count and duration of 10 s.

#### **iv. Mascot database searches**

LTQ-FT MS raw data files were processed to peak lists with *BioworksBrowser 3.2* software (ThermoElectron Corporation). Processing parameters used to generate peak lists were as followed: precursor mass was between 401–5500 Da; grouping was enabled to allow five intermediate MS/MS scans; precursor mass tolerance was set at 5 ppm; minimum ion count in MS/MS was set to 15, and minimum group count was set to 1. Resulting DTA files from each data acquisition were merged and searched against the NCBI or custom databases for identified proteins, using *MASCOT* search engine (Matrix Science Ltd; version 2.2.1; in-house licensed). Searches were done with tryptic specificity, allowing two missed cleavages or “non-specific cleavage” and a mass error tolerance of 5 ppm in MS spectra (i.e. FT-ICR data) and 0.5 Da for MS/MS ions (i.e. LTQ Linear ion trap). Identified peptides were generally accepted only when the *MASCOT* ion score value exceeded 20.

#### **v. Identification of cross-linked peptides**

Mass spectrometric raw files were analyzed via *Thermo Xcalibur* software and peptide peaks of interest were picked manually. A theoretical mass database of potential inter-protein cross-links was built up using a spreadsheet by combining two peptides, which were identified in individual (non-cross-linked) enzymes but missed in the cross-linked enzyme complex by *MASCOT* database search. Additional peptide peaks only found in cross-linked spectra were screened against the mass database. Cross-link candidates were selected by the following rules: trypsin did not cut at the C-terminus of modified lysines or lysines with proline on the C-terminus; up to two missed cleavages were allowed, but non-specific cuttings were not considered; peptide length was 5–30 amino acids; each cross-linked peptide had at least one lysine for cross-linking as well as a lysine or arginine at C-terminus; peaks showed up in at least duplicate experiments; mass error = 5 ppm. Flexible

modifications that might be obtained by oxidation or during SDS-PAGE running were applied to specific residues for identification and the respective mass variations were previously summarized.<sup>6</sup> Identified cross-links were examined by *Mascot* automated target-decoy search against NCBI database to estimate false-discovery rate (FDR) and no protein hits were reported above identity threshold ( $p = 0.05$ ).

#### **vi. Hybrid protein docking**

Global docking and local docking were carried out to solve the structure of the mMDH-CS-Aco complex. In global docking, an automated protein docking web server, *Cluspro* (<http://cluspro.bu.edu/>), was utilized.<sup>7-9</sup> Cross-linked lysines identified by manual search were set as attracting residues. All proteins were treated as rigid bodies with their “open” conformations obtained from crystal structures, giving top 100 ~ 120 structures of highest score based on surface shape complementarity and free energies of desolvation and electrostatic interactions. The crystal structures of Aco, mMDH, and CS were obtained from the Protein Data Bank (PDB ID: 1MLD, 1CTS, and 7ACN). The 24 AA sequences at N-terminus are signal peptides, which are cut off from mature enzymes, so they were excluded from simulation. However, for the recombinant proteins, the FLAG-tag and His-tag were included in model as well as in the final structures. Prior to local docking, all model candidates were screened by *Xwalk* software suite to filter out false positives by distance constraints.<sup>10</sup> Maximum Euclidean distance limit was set to 25 Å, resulting from a combination of DSG spacer arm length (7.7 Å), lysine side chain length (6 Å × 2) and backbone flexibility. In addition to Euclidean distance limit, solvent accessible surface (SAS) distance was set to 30 Å to mimic molecular flexibility of DSG. Solvent radius was 1.4 Å by default and set to 2 Å for SAS distance calculation. Rotamers were removed and only the distance of C $\beta$ -C $\beta$  between two lysines was calculated. A pair of lysines on two proteins in global candidates were considered as a potential cross-link, if their *Xwalk*-calculated separation is no more than the limits.<sup>11</sup> After distance filtering, global candidates bearing at least two potential cross-links were subject to local docking by another protein docking web server, *Rosetta* (<http://rosie.rosettacommons.org/>).<sup>12-14</sup> Derived from each starting global structure, 10 local candidates of lowest interface energy were screened again by *Xwalk*. Final complex structures were chosen based on two criteria: local candidates of lowest interface energy were clustered around a single position on the energy landscape and the structure had the highest number of potential cross-linkers in agreement with experimental results. Interfacial residues in final structures were determined when the measured Euclidean distance was less than 20 Å.

#### **vii. Simulation of electrostatic surface potential**

Prior to simulation, docked structures were modified by *PDB2PQR* web server ([http://nbc-222.ucsd.edu/pdb2pqr\\_2.0.0/](http://nbc-222.ucsd.edu/pdb2pqr_2.0.0/)) to add missing hydrogens and/or heavy atoms and to estimate their titration states.<sup>15,16</sup> Protein complexes were protonated with

favorable hydrogen bonds. Charges and radius were assigned from Amber force field. *PROPKA* was used to predict pK<sub>a</sub> shifts in complexes at pH 7.4.<sup>17</sup> Calculation of surface ESP by Poisson-Boltzmann equation was done by *APBS* web server (<http://www.poissonboltzmann.org/docs/apbs-installation/>)<sup>18,19</sup> with the following parameter settings: water molecules were not removed; no additional ions were added at zero ionic strength; biomolecular dielectric constant was set at 2; and solvent dielectric constant was set at 78.54.

#### d. Kinetic analysis

##### i. Kinetic analysis of the recombinant enzymes

mMDH and CS activity measurements were carried out as in Shatalin *et al.* with some modifications.<sup>20</sup> mMDH was measured for activity with different substrate concentrations for the forward and reverse reactions, in 100 mM potassium phosphate buffer (pH 7.4) in a 96-well plate. L-malate, NAD<sup>+</sup>, oxaloacetate (OAA) and NADH concentrations were varied from zero to 3 mM, 4 mM, 0.1 mM and 0.1 mM, respectively. NADH concentration was measured spectrophotomerically at 340 nm after the addition of 1 nM and 0.1 nM mMDH for the forward and reverse reactions, respectively. CS activity was determined in 100 mM potassium phosphate buffer (pH 7.4) as well, via monitoring the coenzyme A (CoA) production at 412 nm in the presence of 0.2 mM DTNB (5,5'-dithiobis(2-nitrobenzoate)) with 1 nM of enzyme in a 96-well plate. OAA and acetyl coenzyme A (acetyl-CoA) concentrations were varied from zero to 0.5 mM and 0.2 mM, respectively. NADH production/consumption was calculated using the extinction coefficients 6220 M<sup>-1</sup>cm<sup>-1</sup>. Production of citrate can be spectrophotometrically monitored through a subsequent reaction of CoA and DTNB, which yields a di-anion (TNB<sup>2-</sup>) absorbing at 412 nm. Citrate production rate was determined from the maximum linear slope of the curve of absorbance over time. Extinction coefficient of TNB<sup>2-</sup> at 412 nm was 14,150 M<sup>-1</sup>cm<sup>-1</sup>, and the light path length was 0.56 cm. All enzyme concentrations were determined by BCA assay (Thermo Scientific) following the protocol provided by the manufacturer and a SpectraMax M2 (Molecular Devices) was used for absorbance readings. Obtained data was fitted into ordered bi-bi equation in order to calculate the kinetic parameters of the enzymes:

$$v = \frac{v_{max}[A][B]}{K_{iA}K_B + K_B[A] + K_A[B] + [A][B]} \quad (1)$$

##### ii. Coupled activity assays of the mMDH-CS complex in solution with aspartate aminotransferase (AAT) or glycerol

Equal amounts of mMDH and CS were mixed in 10 mM PBS (pH 7.4) to a final total protein concentration of 20 μM, and incubated under gentle shaking at room temperature for 30

min. The coupled activity of the mMDH-CS complex (100 nM) or the crude lysate (0.5 mg mL<sup>-1</sup>) was assayed in a 96-well plate with 1 mM L-malate, 2 mM NAD<sup>+</sup>, 0.1 mM acetyl coenzyme A, 0.2 mM DTNB and 10 mM glutamate in 200 µL of 100 mM potassium phosphate buffer (pH 7.4) in the presence of 1 or 5 U mL<sup>-1</sup> AAT. Control experiments were done without adding AAT. Glycerol was added to the enzyme and substrate solutions to 10% and 20% (v/v) prior to mixing. Then the coupled activity of the mMDH-CS complex (100 nM) or the crude lysate (0.5 mg mL<sup>-1</sup>) was assayed in a 96-well plate with 1 mM L-malate, 2 mM NAD<sup>+</sup>, 0.1 mM acetyl-CoA and 0.2 mM DTNB in 200 µL of 100 mM potassium phosphate buffer (pH 7.4). Control experiments were done without adding glycerol. The absorbance increase at 412 nm was monitored by Synergy™ HTX multi-mode microplate reader (BioTek) over 1 min at 1 s intervals. One unit (U) of enzyme activity was defined as 1 µmole of product formed in one minute.

### **iii. Coupled activity assay of immobilized mMDH-CS complex with AAT**

The mMDH-CS complex solutions (4 µM) and ala-chitosan solution (10 mg mL<sup>-1</sup>) were mixed at a volume ratio of 2:1, and incubated on vortex at room temperature for 15 min. Cross-linked samples were prepared by incubating mixtures of mMDH and CS at 20 µM with 0.2 mM DSG under gentle shaking at room temperature for 30 min, followed by quenching with 2 M Tris (pH 8.3). The cross-linking ratio of DSG:protein was lowered to 10:1 to minimize potential deactivation of enzymes by excessive cross-linkers. 25 µL of the enzyme/polymer suspension was pipetted to the bottom of a polystyrene cuvette (1 cm for light path length) and dried in a vacuum at room temperature for 2 h. Coupled activity of immobilized enzyme complex was assayed in 1 mL of 100 mM potassium phosphate buffer (pH 7.4) containing 1 mM L-malate, 2 mM NAD<sup>+</sup>, 0.1 mM acetyl-CoA, 0.2 mM DTNB, 10 mM glutamate and AAT at 0 or 1 U mL<sup>-1</sup>. The absorbance change at 412 nm was monitored by a UV-Vis spectrophotometer (Evolution 260 Bio, Thermo Scientific).

### **iv. Transient time measurement by fast kinetic study**

Fast kinetic experiment was carried out in a 96-well plate measured by the plate reader equipped with a dual injection module. Before assays, 10 µL of mMDH (20 µM) and 10 µL of CS (20 µM) were mixed in 10 mM PBS (pH 7.4) and incubated under gentle shaking at room temperature for 30 min, followed by dilution to 2 mL in 100 mM potassium phosphate buffer (pH 7.4). The crude lysate was directly used without further dilution. Substrate solution was prepared in 2 mL of potassium phosphate buffer containing 2 mM L-malate, 4 mM NAD<sup>+</sup>, 0.2 mM acetyl-CoA and 0.4 mM DTNB. To setup the assay condition, enzyme and substrate solutions were respectively injected by two separate syringes at a flow rate of 250 µL s<sup>-1</sup>. Total assay volume was 200 µL s<sup>-1</sup> per well. Absorbance at 412 nm was read every 90 ms over 1 min. Transient time of OAA was determined by extrapolating the linear line fitted to the absorbance curve within the first recorded 5 s.

## v. Predicted transient time calculations

In addition to the experimental fast kinetic study of mMDH-CS complex, transient time analysis was performed using the experimentally obtained kinetic parameters of individual recombinant mMDH, recombinant CS and mutant CS(R65A). In Matlab, a function “xprime” was defined as the change in substrate/product concentrations with respect to time and ode45 function was used to solve the differential equations describing these substrate (OAA and acetyl-CoA) consumptions/product (citrate and CoA) formations. Obtained data was fitted using Excel and transient time of OAA was determined by extrapolating the linear line fitted to the time versus product concentration plot. The Matlab code is given below:

```
function xprime = concentrations(t,x);
xprime=[(v0-
((V1*x(1)*x(2))/((KiA*KB)+(KA*x(2))+(KB*x(1))+(x(1)*x(2)))));(-
1)*(V1*x(1)*x(2))/((KiA*KB)+(KA*x(2))+(KB*x(1))+(x(1)*x(2))));(V1*x(1)*
x(2))/((KiA*KB)+(KA*x(2))+(KB*x(1))+(x(1)*x(2))));(V1*x(1)*x(2))/((KiA*
KB)+(KA*x(2))+(KB*x(1))+(x(1)*x(2)))];
```

where x(1) is OAA and x(2) is acetyl-CoA.

## vi. Elasticity coefficient calculations

In order to calculate the elasticity coefficient of CS with respect to OAA, following equation was used (18):

$$\varepsilon_{OAA}^{CS} = \frac{\partial v_{CS}}{\partial [OAA]} \frac{[OAA]}{v_{CS}} \quad (2)$$

where  $v$  is the reaction rate of CS and  $[OAA]$  is the concentration of substrate OAA. After taking the derivative of the rate equation with respect to OAA, kinetic parameters and steady state OAA concentration belonging to CS and CS(R65A) were fitted to the Eq. 2, in order to obtain the steady state elasticity coefficients.<sup>21</sup>

### III. References

- (1) Evans, C. T., Kurz, L. C., Remington, S. J., Srere, P. A., (1996) Active Site Mutants of Pig Citrate Synthase: Effects of Mutations on the Enzyme Catalytic and Structural Properties. *Biochemistry* 35, 10661–10672.
- (2) Alter, G. M., Casazza, J. P., Zhi, W., Nemeth, P., Srere, P. A., and Evans, C. T. (1990) Mutation of essential catalytic residues in pig citrate synthase. *Biochemistry* 29, 7557–7563.
- (3) Altschul, S. F., Madden, T. L., Schäffer, A. A., Zhang, J., Zhang, Z., Miller, W., and Lipman, D. J. (1997) Gapped BLAST and PSI-BLAST: a new generation of protein database search programs. *Nucleic Acids Res.* 25, 3389–3402.
- (4) Martin, G. L., Minteer, S. D., and Cooney, M. J. (2009) Spatial Distribution of Malate Dehydrogenase in Chitosan Scaffolds. *ACS Appl. Mater. Interfaces* 1, 367–372.
- (5) Rogers, G. W., Brand, M. D., Petrosyan, S., Ashok, D., Elorza, A. A., Ferrick, D. A., and Murphy, A. N. (2011) High Throughput Microplate Respiratory Measurements Using Minimal Quantities Of Isolated Mitochondria. *PLoS ONE* (Kowaltowski, A. J., Ed.) 6, e21746.
- (6) Wu, F., and Minteer, S. (2015) Krebs cycle metabolon: structural evidence of substrate channeling revealed by cross-linking and mass spectrometry. *Angew. Chem. Int. Ed.* 54, 1851–1854.
- (7) Comeau, S. R., Gatchell, D. W., Vajda, S., and Camacho, C. J. (2004) ClusPro: a fully automated algorithm for protein-protein docking. *Nucleic Acids Res.* 32, W96–9.
- (8) Comeau, S. R., Gatchell, D. W., Vajda, S., and Camacho, C. J. (2004) ClusPro: an automated docking and discrimination method for the prediction of protein complexes. *Bioinformatics* 20, 45–50.
- (9) Kozakov, D., Beglov, D., Bohnuud, T., Mottarella, S. E., Xia, B., Hall, D. R., and Vajda, S. (2013) How good is automated protein docking? *Proteins: Struct., Funct., and Bioinf.* (Bonvin, A. M. J. J., Janin, J., and Wodak, S. J., Eds.) 81, 2159–2166.
- (10) Kahraman, A., Malmström, L., and Aebersold, R. (2011) Xwalk: computing and visualizing distances in cross-linking experiments. *Bioinformatics* 27, 2163–2164.
- (11) Herzog, F., Kahraman, A., Boehringer, D., Mak, R., Bracher, A., Walzthoeni, T., Leitner, A., Beck, M., Hartl, F.-U., Ban, N., Malmström, L., and Aebersold, R. (2012) Structural Probing of a Protein Phosphatase 2A Network by Chemical Cross-Linking and Mass Spectrometry. *Science* 337, 1348–1352.
- (12) Chaudhury, S., Berrondo, M., Weitzner, B. D., Muthu, P., Bergman, H., and Gray, J. J. (2011) Benchmarking and Analysis of Protein Docking Performance in Rosetta v3.2. *PLoS ONE* (Uversky, V. N., Ed.) 6, e22477.
- (13) Lyskov, S., Chou, F.-C., Conchúir, S. Ó., Der, B. S., Drew, K., Kuroda, D., Xu, J., Weitzner, B. D., Renfrew, P. D., Sripakdeevong, P., Borgo, B., Havranek, J. J., Kuhlman, B., Kortemme, T., Bonneau, R., Gray, J. J., and Das, R. (2013) Serverification of Molecular Modeling Applications: The Rosetta Online Server That Includes Everyone (ROSIE). *PLoS ONE* (Uversky, V. N., Ed.) 8, e63906.
- (14) Lyskov, S., and Gray, J. J. (2008) The RosettaDock server for local protein-protein docking. *Nucleic Acids Res.* 36, W233–8.
- (15) Dolinsky, T. J., Czodrowski, P., Li, H., Nielsen, J. E., Jensen, J. H., Klebe, G., and Baker, N. A. (2007) PDB2PQR: expanding and upgrading automated preparation of biomolecular structures for molecular simulations. *Nucleic Acids Res.* 35, W522–5.
- (16) Dolinsky, T. J., Nielsen, J. E., McCammon, J. A., and Baker, N. A. (2004) PDB2PQR: an automated pipeline for the setup of Poisson-Boltzmann electrostatics calculations. *Nucleic Acids Res.* 32, W665–7.
- (17) Olsson, M. H. M., Søndergaard, C. R., Rostkowski, M., and Jensen, J. H. (2011) PROPKA3: Consistent Treatment of Internal and Surface Residues in Empirical pKa Predictions. *J. Chem. Theory Comput.* 7, 525–537.
- (18) Baker, N. A., Sept, D., Joseph, S., and Holst, M. J. (2001) Electrostatics of nanosystems:

application to microtubules and the ribosome. *PNAS* 98, 10037-10041.

(19) Søndergaard, C. R., Olsson, M. H. M., Rostkowski, M., and Jensen, J. H. (2011) Improved Treatment of Ligands and Coupling Effects in Empirical Calculation and Rationalization of pKa Values. *J. Chem. Theory Comput.* 7, 2284–2295.

(20) Shatalin, K., Lebreton, S., Rault-Leonardon, M., Velot, C., and Srere, P. A. (1999) Electrostatic channeling of oxaloacetate in a fusion protein of porcine citrate synthase and porcine mitochondrial malate dehydrogenase. *Biochemistry* 38, 881–889.

(21) Fell, D. A. (1992) Metabolic control analysis: a survey of its theoretical and experimental development. *Biochem. J.* 286 ( Pt 2), 313–330.